The Laryngoscope

PHR1 Is a Vesicle-Bound Protein Abundantly Expressed in Mature Olfactory Neurons

Bruce Tan, MD; David Brown, MD; Shunbin Xu, PhD; David Valle, MD

Objectives/Hypothesis. To characterize the role of *Phr1*, a gene highly expressed in primary sensory neurons where it encodes an integral membrane protein with an N-terminal pleckstrin homology domain and a C-terminal transmembrane domain, in the olfactory system.

Methods. We studied the immunelocalization of the PHR1 protein in mouse olfactory epithelium both at steady state and during regeneration following methyl bromide (MeBr) exposure using scanning confocal microscopy. Additionally, we examined the electrophysiologic role of *Phr1* in olfaction and short-term olfactory adaptation.

Results. We found that PHR1 is abundantly and specifically expressed in olfactory neurons. It is widely distributed in punctate, vesiculated organelles throughout the cell bodies, axons, and glomeruli of primary olfactory neurons but is specifically excluded from the olfactory cilia. In the regenerating olfactory epithelium, PHR1 expression appears at 14 days following MeBr ablation coinciding with the onset of olfactory neuron maturity. Despite the abundant and specific expression throughout the olfactory neurons, mice lacking *Phr1* did not exhibit differences in the distribution of the components of olfactory signal transduction system, the rate of olfactory regeneration following MeBr exposure, olfactory function, or short-term adaptation to odors.

Conclusions. *Phr1* is widely and abundantly expressed throughout mature olfactory neurons and other primary sensory neurons, but its absence does not appear to affect olfactory morphology, regeneration, sensory function, or adaptation. The exact function of *Phr1* remains to be discovered.

Key Words: PHR1, PLEKHB1, olfaction, maturity, pleckstrin homology, sensory neurons.

***Laryngoscope,* 120:1002–1010, 2010**

INTRODUCTION

Despite recent advances in our understanding of the basic mechanisms and physiology of olfaction, our knowledge of the mechanisms governing neuronal homeostasis in the continuously regenerating olfactory epithelium and the pathophysiology of olfactory dysfunction in humans remains limited. Several neurodegenerative conditions, including Parkinson's disease and Alzheimer's disease, include a prodrome of olfactory dysfunction.[1] Additionally, genetic disorders including Kallmann syndrome,[2] and more recently the Bardet-Biedl syndrome, have been associated with anosmia in humans.[3] However, for the vast majority of patients in whom conductive causes of olfactory loss have been ruled out, the causes of sensorineural olfactory loss are idiopathic and generally attributed to postviral inflammation, inflammation associated with chronic rhinosinusitis, trauma, aging, and tobacco exposure.[1,4] Investigations into the role of aging, tobacco exposure, and trauma (olfactory bulbectomy) in animal models demonstrated that a shift in the balance of neurogenesis and apoptosis toward apoptotic cell death through caspase-3–mediated pathways in the olfactory neuroepithelium was the likely cause of olfactory loss in those affected populations.[5–7] Conversely, yet unknown derangements in selection, maturation, and apoptotic control of olfactory neurons are thought to give rise to olfactory neuroblastoma[8] and demonstrate the need for an improved understanding of olfactory neuronal homeostasis in human disease.

Seeking to identify genes preferentially expressed in the retina, Xu et al. identified *PHR1* in a differential hybridization screen of an arrayed human retinal cDNA library compared against a probe derived from human fibroblast RNA. *PHR1* was subsequently found to have two promoters and alternative splicing of an internal exon to produce four specific transcripts. All four *PHR1*

From the Department of Otolaryngology–Head and Neck Surgery (B.T., D.B.), the Howard Hughes Medical Institute (D.V.), McKusick-Nathans Institute of Genetic Medicine (D.V.), Johns Hopkins University School of Medicine, Baltimore, Maryland; and the Department of Ophthalmology and Neurological Sciences, Rush University Medical Center, Chicago, Illinois (S.X.), U.S.A.

Editor's Note: This Manuscript was accepted for publication October 14, 2009.

Presented at the AAO-HNSF Annual Meeting, Washington, DC, U.S.A., September 16, 2007.

This work was supported in part by a grant from the Foundation for Fighting Blindness (d.v.). Dr. David Valle was an investigator in the Howard Hughes Medical Institute at the time of this study. Dr. Bruce Tan was a Johns Hopkins Otolaryngology resident supported by a research training program sponsored by the Greater Baltimore Medical Center.

Send correspondence to David Valle, MD, McKusick-Nathans Institute of Genetic Medicine, Broadway Research Building, 519, Baltimore, MD 21287. E-mail: dvalle@jhmi.edu

DOI: 10.1002/lary.20779

mRNA splice forms encode isoforms with a pleckstrin homology (PH) domain at the N-terminus and a transmembrane domain at the C-terminus. Only splice forms 3 and 4 are expressed outside the retina.[9] Although PH domain-containing proteins are best known for their ability to target binding partners to cellular membranes by binding phosphoinositides in phosphoinositide 3-kinase signaling, studies have shown that PH domains also play a significant role in binding the $\beta\gamma$ subunits of heterotrimeric G proteins.[10] Physiologically, PH domain-containing proteins are involved in cellular signaling, cytoskeletal organization, and membrane trafficking.[11] To date, PHR1 remains the only described integral membrane protein with a PH domain.

To study the role of PHR1 in vivo, Xu et al. produced a *Phr1* knockout mouse that disrupted the *Phr1* gene by inserting a β-galactosidase reporter gene downstream of the *Phr1* promoter.[12] In analyzing the phenotype of these mice, they unexpectedly found expression of *Phr1* in primary sensory neurons of the olfactory, tactile, and auditory systems. In fact, they found that levels of *Phr1* expression in the olfactory epithelium were equivalent to or exceeded those in the retina and brain. Despite the high level of *Phr1* expression in the olfactory system, no overt olfactory deficits were observed in mice with a complete deficiency of *Phr1*. In an independent study by Krappa et al., who referred to *Phr1* as *evt-1*, localized PHR1 protein to the retinal post-Golgi compartment in frog photoreceptors and suggested a role for PHR1 as a mediator of post-Golgi trafficking.[13]

In yeast two-hybrid experiments, Etournay et al. found interactions between PHR1 and two unconventional myosins—myosin Ic and myosin VIIa—found in the middle ear. Because both of these unconventional myosins are implicated in slow adaptation in mechanotransduction of auditory hair cell bundles,[14] the authors suggested that PHR1 was involved in this process. Additionally, experiments in our laboratory suggested that certain isoforms of PHR1 dimerize and form heterodimers with carboxypeptidase E in the retina and RGS9s in the brain (Xu et al. unpublished data). Because both of these proteins are involved in light adaptation within the retina, these results suggest a role for PHR1 in the adaptive processes of sensory neurons. In a separate study, Colin et al., using subtractive hybridization, demonstrated that *PHR1* (referred to in their paper as *PLEKHB1*) was one of the genes that defined noninvasive and more differentiated forms of brain tumors.[15] These results reinforced our evidence that *PHR1* plays an important but undescribed role in terminally differentiated sensory neuron biology.

In this study, we sought to further examine the role of *Phr1* in the mouse olfactory system in vivo. We used immunofluorescence to determine the subcellular location of PHR1 and its functions. We also observed the effect of PHR1 on the distribution of other membrane-bound components of the olfactory signal transduction system. Given the unique capacity of the olfactory system for continuous turnover and regeneration following injury, we studied the possible role of PHR1 in the survival and regeneration of olfactory neurons. Using electro-olfactograms (EOGs), we also examined the role of PHR1 in olfactory function and adaptation.

MATERIALS AND METHODS

Mouse Genotyping and Handling

To study the role of PHR1, Xu et al. had previously produced a *Phr1* knockout-knockin construct that targeted exon 3 *Phr1* and inserted a β-galactosidase reporter and neomycin resistance construct downstream and under the control of the *Phr1* promoter.[12] This construct was designed to disrupt the expression of all four isoforms of PHR1, including the retinal long form. We genotyped pups from heterozygous $Phr1^{\beta gal/+}$ breeding pairs with a Southern blot protocol previously established.[8] Genotyped wild-type $Phr1^{+/+}$ and knockout $Phr1^{\beta gal/\beta gal}$ mice were then identified and used for this study. All mouse matings and manipulations were carried out according to Association for Assessment and Accreditation of Laboratory Animal Care International guidelines at the Johns Hopkins University School of Medicine. All protocols have been reviewed and approved by the Johns Hopkins University Institutional Review Board.

Antibodies and Immunohistochemistry

Tissue preparation. We anesthetized mice with ketamine-xylazine and perfused them with intracardiac phosphate buffered saline and 4% paraformaldehyde fixative (Sigma, St. Louis, MO). Following fixation, the dissected mouse tissue was decalcified with 30% sucrose plus 250 mM ethylenediaminepentaacetic acid (EDTA) (Sigma) for 48 hours at 4°C, frozen in Tissue-Tek Optimal Cutting Temperature (OCT) Compound (Ted Pella, Redding, CA), and cut into 10-μm sections on a cryostat.

Immunofluorescence. For immunofluorescence, we hydrated cryostat sections in phosphate buffered saline (PBS) plus 10% normal serum (Sigma) for 15 minutes and permeabalized the sections with PBS with 1% Triton (Sigma) plus 10% normal serum (Buffer A) three times for 5 minutes each. We then applied the primary antibody in PBS with 1% Triton plus 10% normal serum and incubated the sections overnight at 4°C. We used the primary antibodies at the following dilutions: rabbit anti-mouse PHR1 at 1:500, rabbit anti-mouse ACIII at 1:1000, rabbit anti-mouse $G_{\gamma 13}$ at 1:500, rabbit anti-mouse $G_{\alpha olf}$ at 1:250, rabbit anti-mouse TuJ1 at 1:500, goat anti-mouse olfactory marker protein (OMP) at 1:500, and donkey anti-mouse acetylated tubulin at 1:1000. (ACIII, $G_{\gamma 13}$, $G_{\alpha olf}$, TuJ1, OMP at 1:500, and acetylated tubulin antibodies were kind gifts of the lab of Dr. R. Reed.) We visualized the primary antibody using the appropriate Alexa488 or Alexa594 (Molecular Probes, Invitrogen, Carlsbad, CA) fluorophore labeled secondary antibody. Nuclei were visualized with the DNA stain 4′,6-diamidino-2-phenylindole (DAPI) (Molecular Probes, Invitrogen). All images were collected on a Zeiss LSM 510 scanning confocal laser scanning microscope (Carl Zeiss AG, Oberkochen, Germany).

Electron microscopy. Nasal turbinates were harvested from freshly sacrificed mice and fixed in PBS with 4% paraformaldehyde, 0.1% glutaraldehyde, and 2 mM $MgCl_2$ for 1 hour (Sigma) and decalcified overnight at 4°C in decalcifying buffer (0.1 M EDTA, 2.5% glutaraldehyde, 0.1 M sodium cacodylate buffer at pH 7.2). The turbinate tissue was then washed in PBS and submitted to the Johns Hopkins microscopy core laboratory for ultrathin sectioning and standard transmission electron microscopy. Per their protocol, the samples were postfixed in a 0.8% potassium ferrocyanide solution in the dark. After a brief D-H2O rinse, samples were placed in 2% uranyl acetate for 1 hour in the dark. Following en bloc staining, cells were dehydrated through a graded series of ethanol solutions and embedded in Spurr's low viscosity resin (Polysciences Inc.

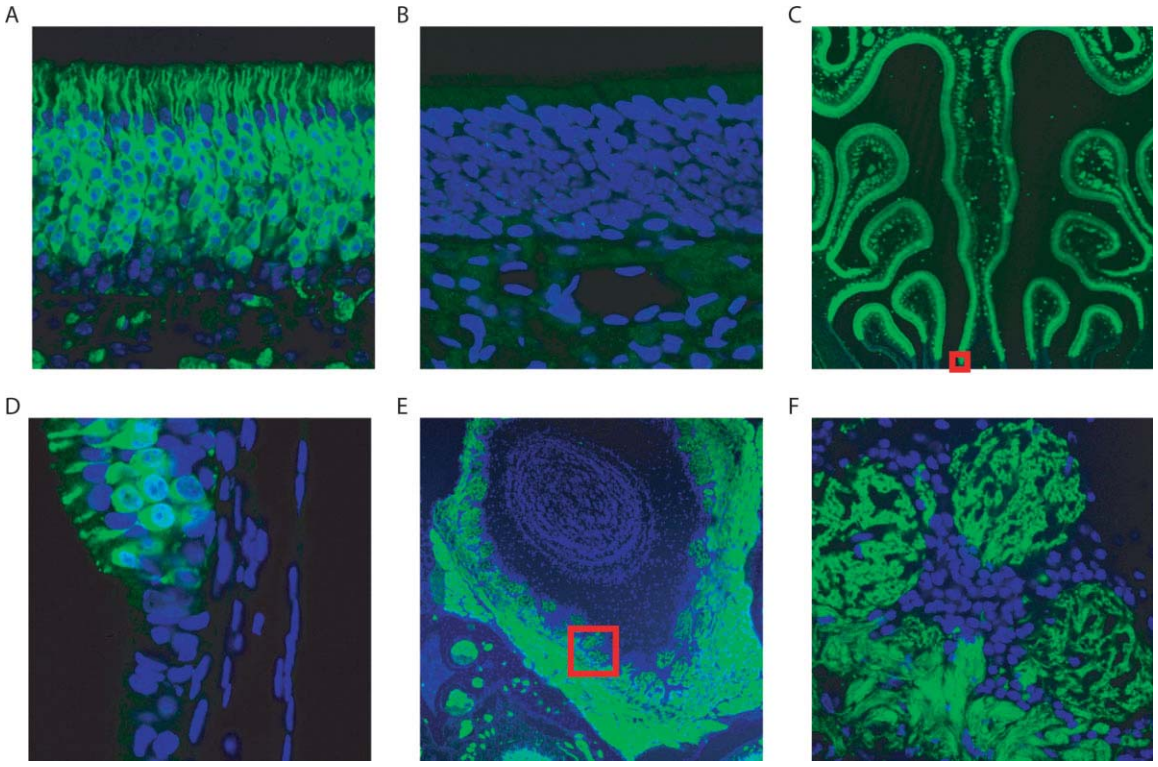

Fig. 1. Distribution of PHR1 protein in olfactory tissue. Coronal tissue sections of olfactory epithelium were immunostained with polyclonal antibodies to PHR1 and secondarily labeled with Alexa-fluor 488 secondary antibodies (green). Nuclei are counterstained with 4′,6-diamidino-2-phenylindole (blue). (A) PHR1 protein is expressed throughout olfactory neuron soma and apical dendrites and (B) is absent in a similarly prepared *Phr1*$^{\beta gal/\beta gal}$ section. (C) A low-power view demonstrating PHR1 has a widespread distribution throughout the main olfactory epithelium that does not extend to the respiratory epithelium. (D) Detail of area highlighted in (C) demonstrating a magnified view of the transition between olfactory and respiratory epithelium. (E) Within the olfactory bulb, PHR1 is found in primary olfactory neurons in the axonal layer and extends to synapses in the olfactory glomeruli. (F) Detail of the area highlighted in (E) demonstrating a magnified view of an olfactory glomeruli and the absence of PHR1 staining in the plexiform layer. [Color figure can be viewed in the online issue, which is available at www.interscience.wiley.com.]

Warrington, PA) and cured at 60°C for 2 days. Sections were cut on a Riechert Ultracut E (Depew, NY) with a DiATOME diamond knife (Hatfield, PA). Sections measuring 80 nm were picked up on Formvar-coated 1 × 2 mm copper slot grids and stained with uranyl acetate followed by lead citrate. Grids were viewed on a Hitachi 7600 transmission electron microscope (Hitachi, Tokyo, Japan) operating at 80 kV, and digital images were captured with an AMT (Advanced Microscopy Techniques, Danvers, MA) 1 k × 1 k charge-coupled device camera.

Methyl Bromide Ablation of Olfactory Epithelium

Methyl bromide (MeBr) ablation was carried out according to protocols previously described by Schwob et al.[16] Briefly, 6-week-old *Phr1*$^{+/+}$ and *Phr1*$^{\beta gal/\beta gal}$ mice were placed in a wire enclosure measuring 15 × 15 × 15 cm and centered in a 30 × 30 × 30 cm Plexiglas box and exposed to MeBr gas at 330 ppm in purified air at a flow rate of 10 L/min. The duration of exposure was 5 hours. The mice were sacrificed at the indicated intervals (n = 3 in each group at each time point). Cryosection of the olfactory system for immunofluorescent analysis was previously described. We obtained the shown images from a standardized portion of septal olfactory epithelium.

Electro-olfactogram Recordings

The stock odorants amyl acetate, acetophenone, and heptanal (kind gift of Dr. R. Reed) were diluted in water to the indicated concentrations. Two milliliters of odorant solution were placed in a sealed 10-mL glass test tube and allowed to equilibrate in the vapor phase. The vapor was delivered as a 0.1-second pulse into a continuous stream of humidified air flowing across the tissue surface. All experiments were recorded using two electrodes placed on turbinates IIb and III of freshly harvested mouse heads (n = 5). The data were analyzed with Clampfit (Axon Instruments, Sunnyvale, CA) and the peak heights were determined from prepulse baselines. Due to variability in the magnitude of the recordings resulting from electrode placement, the EOG data was normalized to the recording obtained from that obtained from amyl acetate at 10^{-4} M.

For the adaptation experiments, sequential pulses of amyl acetate (10^{-4} M) odorant were generated at progressively longer intervals following the initial odorant pulse starting at 1 ms of separation. The magnitude of the response to the second odorant pulse was normalized to that obtained from the initial odorant pulse.

RESULTS

PHR1 Localization in Olfactory Neurons

In wild-type mice, immunolocalization in the olfactory epithelium showed abundant PHR1 protein within primary olfactory neurons (Fig. 1A). As expected, immunostaining of the *Phr1*$^{\beta gal/\beta gal}$ specimens showed no staining (Fig. 1B). Olfactory neurons exist within a pseudostratified neuroepithelium sandwiched between an

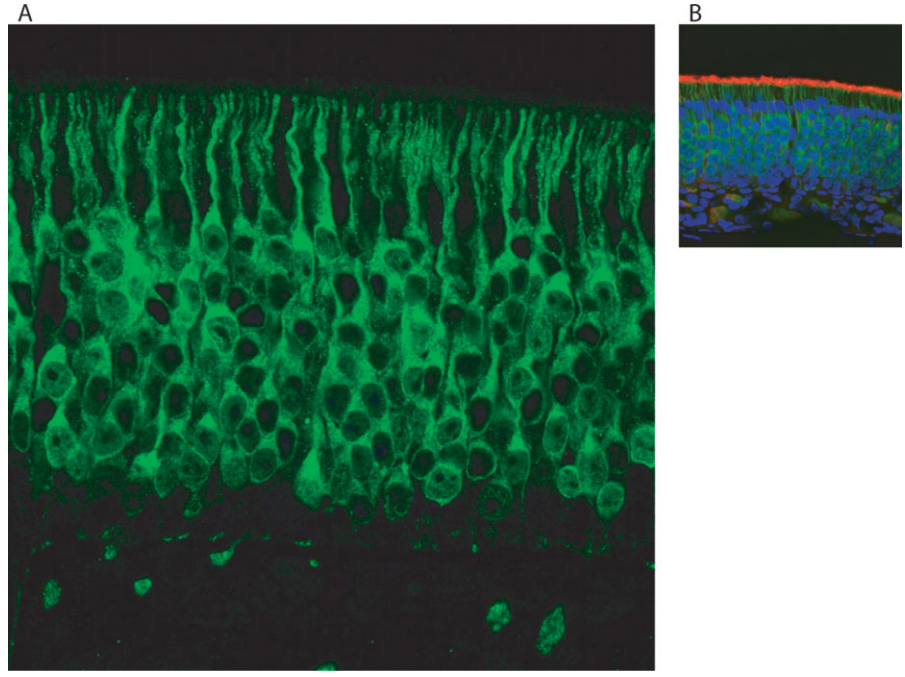

Fig. 2. High-power confocal scanning microscope section of olfactory epithelium. Coronal tissue sections of olfactory epithelium were immunostained with polyclonal antibodies to PHR1 and secondarily labeled with Alexa-fluor 488 secondary antibodies (green). Monoclonal antibodies to acetylated tubulin are secondarily labeled with Alexa-fluor 594 antibodies (red). (A) Punctate distribution of PHR1-bearing vesicles can be seen throughout olfactory neurons with increased density seen in the apical juxtanuclear region. (B) PHR1-bearing vesicles extend to apical dendrite, but olfactory cilia do not appear to contain measurable PHR1 as evidenced by the absence of costaining with acetylated tubulin. [Color figure can be viewed in the online issue, which is available at www.interscience.wiley.com.]

apical layer, containing non-neural supportive sustentacular and microvillar cells, and a basal stem cell layer containing the globose basal cells and the horizontal basal cells. None of these surrounding cell layers appear to contain PHR1 protein. Additionally, PHR1 was specific to neuronal tissue (Fig. 1C) with no expression seen in the adjacent portions of ciliated respiratory epithelium (Fig. 1D). In the olfactory bulb, PHR1 is observed in the glomerular layer of the olfactory epithelium but does not extend into the interneurons of the plexiform layer (Fig. 1E and 1F).

Within the olfactory neurons, PHR1 appears on tiny punctate intracellular vesicles that are distributed throughout the soma, apical dendrites, dendritic knobs, and basal axons extending toward the olfactory bulb (Fig. 2A). There is enrichment of PHR1 protein in the apical juxtanuclear portion of the cytoplasm corresponding to the location of the Golgi apparatus in electron micrographs and immunostaining of olfactory epithelium (see supplementary Appendix). Interestingly, although large numbers of the PHR1-bearing vesicles are present within the dendritic knobs, there is little or no PHR1 protein on the plasma membranes of the olfactory cilia, and there is no staining of the ciliary layer of the olfactory epithelium (Fig. 2B).

Distribution of the Components of Olfactory Signal Transduction

The distribution of PHR1 in punctate vesicular intracellular organelles concentrated over the Golgi apparatus is suggestive of a role for *Phr1* in olfactory neuron protein trafficking. In olfactory signal transduction, odorants couple with specific odorant receptors on the surface of olfactory cilia. This interaction triggers coupling with $G_{\alpha olf}$, which releases the soluble G_{β} and $G_{\gamma 13}$ subunits. The activated $G_{\alpha olf}$ stimulates type III adenylate cyclase to produce cAMP, which in turn triggers cyclic nucleotide-gated channel-induced depolarization.[13] We examined the distribution of membrane-bound signaling components of type III adenylate cyclase, $G_{\alpha olf}$, and $G_{\gamma 13}$ in *Phr1* wild-type and $Phr1^{\beta gal/\beta gal}$ animals and found no differences in the intracellular distribution of these signal transduction components. Type III adenylate cyclase (Fig. 3A) and $G_{\gamma 13}$ (Fig. 3C) were concentrated in the neurosensory cilia with weak staining seen along the apical juxtanuclear soma likely corresponding to signal transduction components within the Golgi and post-Golgi compartments. $G_{\alpha olf}$ was distributed more evenly throughout the olfactory neurons with punctate staining within the soma and axons of olfactory neurons similar to PHR1 (Fig. 3B). Unlike PHR1, however, $G_{\alpha olf}$ was also present within the olfactory neurociliary layer.

Recovery of PHR1 Expression Following Methyl Bromide Ablation

The capacity for continuous neurogenesis within the olfactory epithelium provided a unique opportunity to examine olfactory neurogenesis in *Phr1*-deficient animals. The ability for passive inhalation of the selective olfacto-toxic MeBr gas to destroy >95% of the olfactory epithelium and the subsequent ability for the olfactory epithelium to reconstitute is well described in numerous previous studies. We sacrificed MeBr treated animals 48 hours, 7, 14, and 30 days after the treatment and examined the PHR1 expression pattern during the regeneration along with a pan-neuronal marker TuJ1 and OMP, a marker for olfactory neuron maturity.

Forty-eight hours following exposure to MeBr, both *Phr1* wild-type and $Phr1^{\beta gal/\beta gal}$ animals had almost complete ablation of their sustentacular cell layer and olfactory neuroepithelium. Both groups of animals exhibited a similar rate of regeneration of the olfactory neuroepithelium as

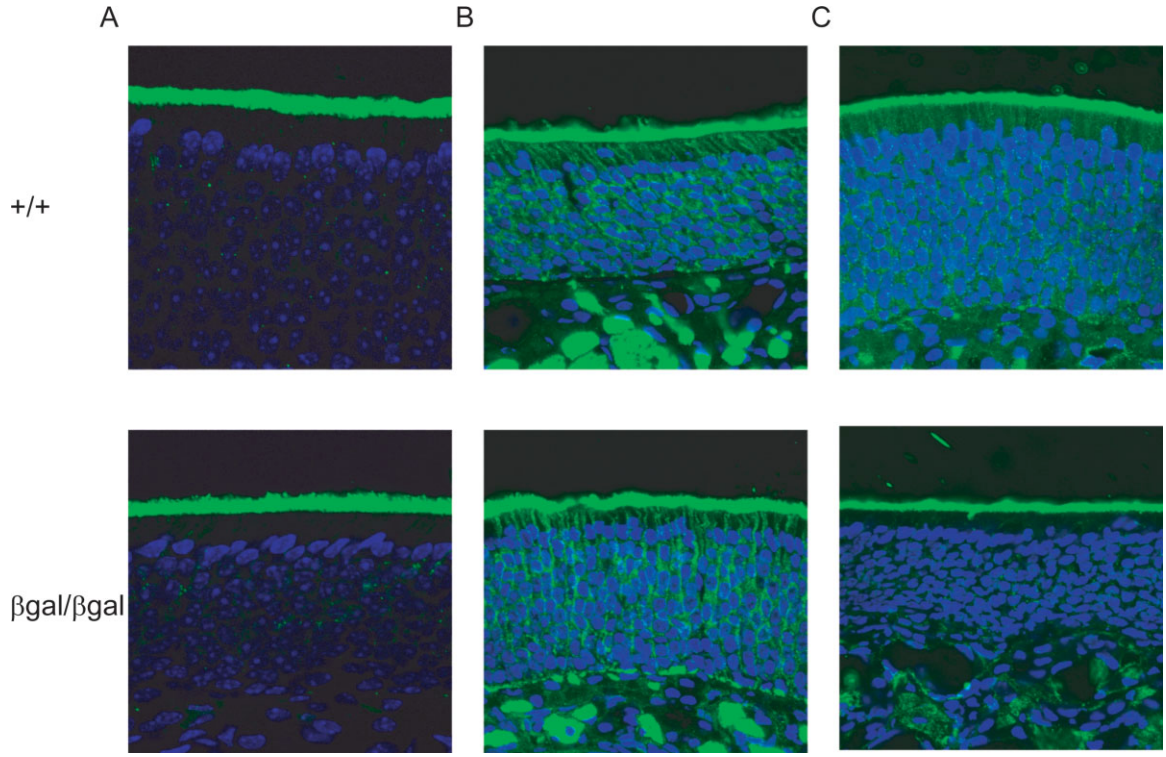

Fig. 3. Distribution of olfactory protein localization in *Phr1*$^{+/+}$ and *Phr1*$^{\beta gal/\beta gal}$ mice. Sections of olfactory epithelium were immunostained with antibodies to olfactory cilia-enriched signal transduction components (ACIII, $G_{\alpha olf}$ and $G_{\gamma 13}$). Nuclei are counterstained with 4′,6-diamidino-2-phenylindole. The distribution of (A) ACIII, (B) $G_{\alpha olf}$, and (C) $G_{\gamma 13}$ appears to be unperturbed in *Phr1*$^{\beta gal/\beta gal}$ animals. [Color figure can be viewed in the online issue, which is available at www.interscience.wiley.com.]

assessed by return of TuJ1 and OMP staining. TuJ1 positive cells were first identified along the basal cell layers at 7 days following MeBr exposure, whereas a single layer of OMP positive cells are first identified at 14 days. At 30 days following MeBr exposure, both *Phr1* wild-type and *Phr1*$^{\beta gal/\beta gal}$ animals were able to restore a histologically normal olfactory epithelium with mature olfactory neurons and an apical layer of sustentacular cells (Fig. 4A–4E and Supporting Appendix).

The PHR1 containing olfactory neurons were completely ablated following exposure to MeBr (Fig. 4A, preexposure; Fig. 4B, 48 hours postexposure). PHR1 protein in olfactory neurons was not observed at 7 days after MeBr exposure (Fig. 4C), but at 14 days postexposure a thin layer of PHR1 expressing olfactory neurons was observed (Fig. 4D). The thickness of the PHR1 containing the sensory layer continued to increase through day 30 when a morphologically normal olfactory layer was restored (Fig. 4E). Interestingly, the return of PHR1 containing neurons at 14 days post-MeBr (Fig. 4F) coincided exactly with that of OMP (Fig. 4G). Indeed, double-stained sections of regenerating olfactory epithelium at 14 days showed almost complete overlap of the PHR1 and OMP containing mature olfactory neurons (Fig. 4H), suggesting that *Phr1* expression demarcates the onset of olfactory neuron maturity.

Electrophysiologic Recordings

We recorded and compared EOGs generated from olfactory epithelium of wild-type and *Phr1*-null mice evaluating them for odor response, recovery, and short-term adaptation. Response magnitudes following exposure to stock odorants of amyl acetate, heptanal, and acetophenolate at varying concentrations were normalized to the response generated from aliquots of equilibrated amyl acetate at 10^{-4} M (Fig. 5A). We found no statistically significant differences between normalized EOG response magnitudes in wild-type and knockout animals for the odorants tested.

To evaluate recovery following odor exposure, we calculated the time taken for the olfactory epithelium surface potential to recover to half the maximum depolarization potential following odor stimulus generated from aliquots of 10^{-4}M amyl acetate. Both wild-type and knockout mice showed equivalent recovery times following odor stimulation (494 ms and 462 ms, respectively; $P = .347$).

We also evaluated the role of *Phr1* in olfactory short-term adaptation to odor stimuli. EOG recordings were made following sequentially pulsed odorant stimuli at increasing time intervals. Comparing the ratio of the depolarization potential generated following the second stimulus to the initial depolarization potential, we found no differences between the adaptive responses of *Phr1* wild-type and knockout animals (Fig. 5B).

DISCUSSION

In these studies, we characterized the distribution of PHR1 in the murine olfactory epithelium. We find PHR1 widely distributed throughout virtually all mature, primary olfactory neurons extending from the

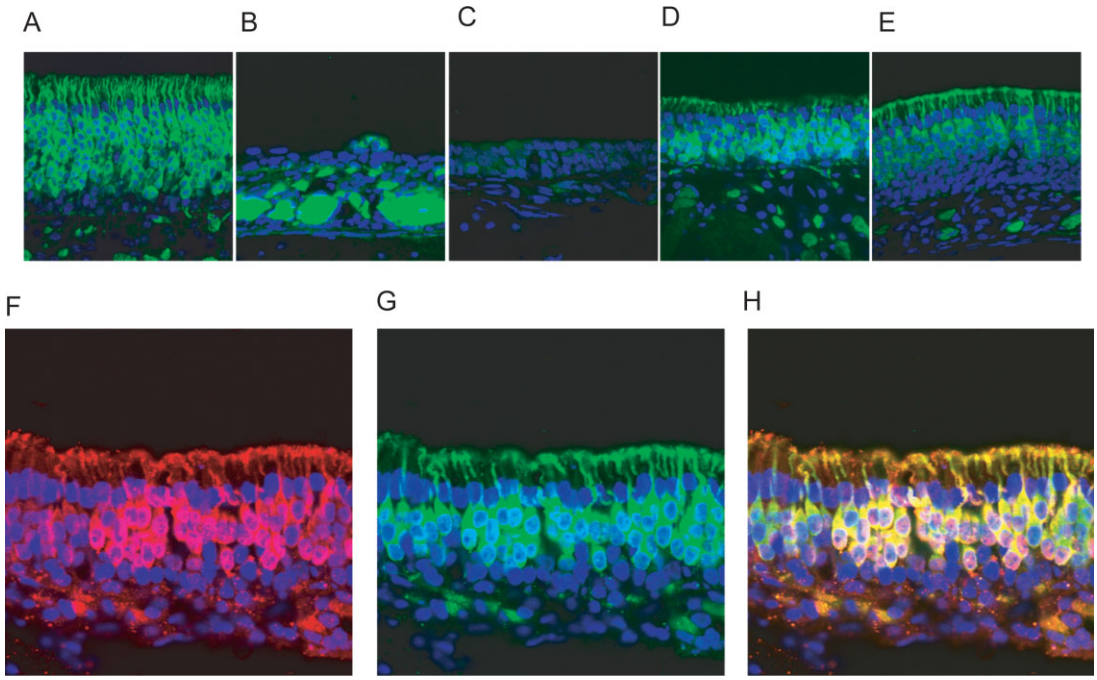

Fig. 4. PHR1 expression reappears in the olfactory epithelium treated with methyl bromide (MeBr) coinciding with olfactory neuron maturity. Coronal tissue sections of olfactory epithelium were immunostained with polyclonal antibodies to PHR1 and secondarily labeled with Alexa-fluor 488 secondary antibodies (green). Monoclonal antibodies to olfactory marker protein (OMP) are secondarily labeled with Alexa-fluor 594 antibodies (red). *Phr1*$^{+/+}$ mice were treated with an olfactory neuron specific toxin, MeBr, and sections were obtained at (A) pretreatment, (B) 48 hours, (C) 7 days, (D) 14 days, and (E) 30 days following treatment. (F) At 14 days after exposure, OMP expressing mature olfactory neurons are first detected along with (G) PHR1 expressing neurons. (H) Costaining of OMP and PHR1 showing synchronous presence of OMP and PHR1 in mature olfactory neurons. [Color figure can be viewed in the online issue, which is available at www.interscience.wiley.com.]

dendritic knob, down the apical dendrite toward the soma, and along the basal axons extending to the synapses within the glomeruli of the olfactory bulb (Fig. 1). The punctate pattern visualized in our images is demonstrative of the presence of PHR1 on vesicles being transported throughout olfactory neurons (Fig. 2).

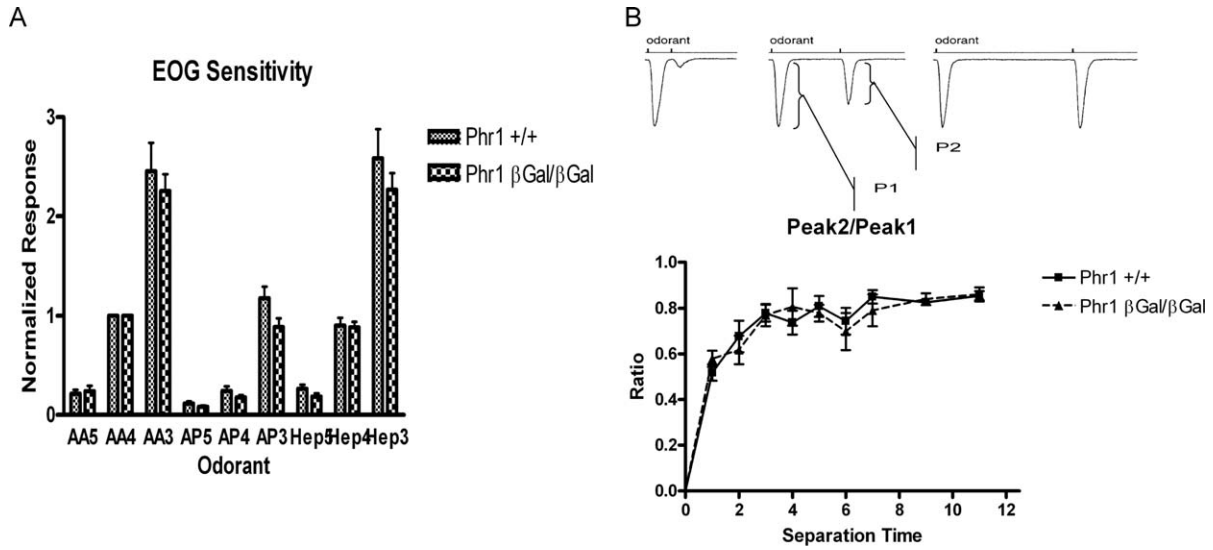

Fig. 5. Olfactory responses of *Phr1*$^{\beta gal/\beta gal}$ mice. The olfactory epithelia of 6-week-old wild-type and *Phr1*$^{\beta gal/\beta gal}$ mice were exposed to either single or sequential brief pulses of vapor-phase odorants and electro-olfactograms (EOGs) were recorded. Three odorants—amyl acetate (AA), acetophenone (AP), and heptanal (Hep)—were tested over a three-log range of concentrations. Short-term adaptation (STA) was assessed by recording EOGs from olfactory epithelium stimulated with sequentially pulsed odorants separated by increasing intervals. (A) Graphical representation of the average normalized responses recorded from the olfactory epithelium after stimulation from a single pulse of odorant showing similar responses in wild-type and *Phr1*$^{\beta gal/\beta gal}$ mice. Raw responses were normalized to the averaged response to AA at 10^{-4} M. (B) Graphical representation of the response obtained in response to the second pulse expressed as a ratio of the response obtained from the initial odorant pulse showing equivalent STA in wild-type and *Phr1*$^{\beta gal/\beta gal}$ mice. Data shown are mean ± standard deviation for responses from five independent recordings.

Indeed, electron micrographs of primary olfactory neurons show a high density of vesicle-like structures found throughout the soma and apical dendrites (see supplementary Appendix). These data support the model of PHR1 as an integral membrane protein and correlate with previous findings that used density gradient fractionation to localize PHR1 to the post-Golgi compartment of frog photoreceptors.[13] Interestingly, the olfactory cilia appear to have significantly lower amounts of PHR1, suggesting that PHR1 and its PH domain likely does not play a direct role in the initial signal transduction events following odorant binding to the olfactory receptor.

In mature primary olfactory neurons, dendritic knobs give rise to multiple sensory cilia that project into the nasal mucosa. The membrane surfaces of these cilia are highly enriched in the components of olfactory signal transduction and enable the detection of odors. Odorant signal transduction is initiated by odorant binding to an olfactory receptor belonging to a large family of G-protein coupled receptors, leading to activation of the olfactory G-protein heterotrimer.[17,18] The G-protein heterotrimer consists of an alpha-subunit $G_{\alpha olf}$ and a $\beta\gamma 13$-subunit. The activation of $G_{\alpha olf}$ leads to stimulation of type III adenylate cyclase, the subsequent opening of cyclic nucleotide gated calcium channels causing depolarization of the ciliary membrane. We find normal enrichment of these critical components of signal transduction in the olfactory cilia of *Phr1*-knockout animals suggesting that despite the absence of PHR1, trafficking of signal transduction molecules proceeds normally (Fig. 3). Surface electrophysiologic recordings utilizing an EOG supports the notion that PHR1 is unlikely to play a role in olfactory signal transduction because surface potentials recorded using different odorants and in short-term adaptation were unchanged when comparing wild-type and *Phr1*-knockout animals, although more specific testing utilizing direct neuronal measurements via patch clamping will be one of the goals of future experiments.

Although observations suggest a highly regulated intracellular mechanism for trafficking and subcellular localization of proteins in olfactory neurons, little is known about the mechanisms by which these processes are regulated. Several recent studies suggest that selecting proteins for entry into the olfactory ciliary compartment is tightly regulated at the basal bodies located in the dendritic knobs. The absence of *CNGB1*, a member of the heterotrimeric cyclic nucleotide gated cation channel, results in subciliary accumulation of the remaining components of the CNG channel, suggesting that mechanisms at the basal body selectively exclude entry of incomplete CNG channels into the ciliary compartment.[19] The mediators underlying the selectivity of the olfactory ciliary compartment are only beginning to be understood. CEP290, a protein found in dendritic knobs and thought to be involved in ciliary cargo sorting, was recently shown to selectively allow transport of G-proteins into the ciliary space.[20] Elucidating the mechanisms by which integral proteins gain entry into the ciliary compartment is an area of active investigation.[21] The current model for ciliary trafficking suggests that ciliary-bound integral proteins have specific cytoplasmic sequences that facilitate binding to specialized intraflagellar particles that attach to an anterograde motor that drives these proteins into the ciliary compartment.[22] PHR1, although abundantly present in the post-Golgi vesicles, appears to be excluded from the ciliary membrane. Whether PHR1 plays a specific role in ensuring ciliary exclusion or is selectively excluded from ciliary trafficking by proteins such as CEP290 remains worthy of investigation.

In the maturation process of globose and horizontal basal stem cells into mature, functional olfactory neurons, several events are known to take place. Globose and horizontal basal stem cells first differentiate into progenitor cells of olfactory receptor neurons, each of which expresses a single olfactory receptor. The process by which each developing neuron selects a single receptor from up to 1,000 olfactory receptor genes distributed throughout the genome remains an area of active investigation.[18] Upon selection of an olfactory receptor, an apical dendrite projects through the sustentacular cell layer to insert sensory cilia into the ciliary layer, and a basal axon targets to the few specific glomeruli in the olfactory bulb that receives input from other olfactory neurons bearing the identical olfactory receptor.[17] Maturity is thought to occur once a successful synapse occurs within the olfactory bulb. The molecular mechanisms that govern and regulate this process have, to date, not been elucidated, but maturity is associated with expression of OMP in olfactory neurons.[23]

OMP is a cytoplasmic protein that is first expressed on embryonic day 14 in mice. This time period coincided with the establishment of synaptic connection of primary olfactory neurons with the olfactory bulb, and as a result OMP is extensively used as a surrogate marker for olfactory neuron maturity.[24] Despite its abundant expression in primary olfactory neurons throughout the soma, cilia, dendrites, and basal axons, the function of OMP still remains unknown. OMP-deficient mice demonstrate a mild to moderate decrease in their maximal response to odor stimuli and altered recovery kinetics following odorant exposure.[25] Despite these observations, behavior testing revealed that OMP-deficient mice did not differ from controls in their ability to discriminate odors but had an expected elevation in odorant thresholds needed to alter behavior.[26] On a morphological level, OMP-deficient mice are indistinguishable from their wild-type counterparts with equivalent ratios of mature and immature neurons. Subtler abnormalities have, however, been observed in the developing olfactory bulbs of OMP-deficient animals with occasional primary axons overshooting the glomerular layer and extending into the external plexiform layer. This aberrant axons targeting, however, rectifies by the time the animals are 5 weeks in age.

At first glance, PHR1 and OMP exhibit many similarities in that they are both abundantly expressed and widely distributed throughout mature olfactory neurons. Despite the abundance of OMP throughout olfactory neurons, studies of OMP-knockout mice are viable and

exhibit only subtle abnormalities in olfaction. Like *OMP, PHR1* expression is also confined to mature olfactory neurons and may indeed prove useful in the study of olfactory neuron development. Given the synchronous return of PHR1 and OMP in regenerating MeBr ablated mucosa (Fig. 4), it appears likely that the regulatory program triggering the expression of *Omp* and *Phr1* upon olfactory neurons maturity is intertwined. Interestingly, both genes are located within 3 Mb of each other in humans (chromosome 11) and mice (chromosome 7). However, unlike OMP, which is a cytosolic protein, PHR1 is an integral membrane protein that is found on vesicle-like organelles in olfactory neurons. As a result, it appears that OMP is able to diffuse into the cytosolic core of the olfactory cilia, whereas PHR1 is excluded. Furthermore, whereas *OMP* expression is specific to the olfactory system, *PHR1* is also found in many other sensory neuron types.

Our studies also illustrate the prominent and widespread distribution of PHR1 in the olfactory epithelium and the synchrony of *Phr1* expression with olfactory neuron maturity. Indeed, subtractive hybridization studies comparing pilocytic astrocytomas and glioblastoma multiforme have revealed that *PHR1* expression was significantly higher in the better differentiated, less aggressive pilocytic astrocytoma samples when compared with the dedifferentiated, more aggressive glioblastoma multiforme samples. This study reinforces our finding that PHR1 is a marker for terminally differentiated neural tissue and that failure to reach terminal differentiation prevents the expression of *PHR1*. It would be interesting to see if such a correlation can be found in olfactory neuroblastoma.

Together, these studies suggest that even though PHR1 is widely distributed throughout the olfactory epithelium, its absence has minimal or subtle influences on sensory function, but its expression is synchronous with olfactory neuron maturity. Several possible explanations for this observation include: 1) PHR1 is unrelated to olfactory neuron sensory function and neuronal maturation and instead has a function related to neuronal homeostasis that we have yet to test, 2) PHR1 has a subtle influence of sensory function that only more precise measures using patch clamp techniques can delineate, or 3) a redundant gene such as PHR1's closest homologue, designated Evt-2 by Krappa et al., takes on the role of PHR1 with little functional deficit. Evt-2 has an overall 38.4% amino acid and a 57.6% sequence identity to PHR1 isoform 3.[12] Its expression pattern in tissue, however, is not restricted to primary sensory neurons and is also found in tissues such as the heart, kidney, lung, and muscles. Although Northern blot analysis of the olfactory epithelium of *Phr1*-null mice do not show increases in the expression of Evt-2, the only way to exclude this possibility is through the construction of a *PHR1/Evt-2* double knockout mouse.

CONCLUSION

PHR1 is specifically expressed in terminally differentiated olfactory neurons and may contribute to the normal functions of the mature olfactory neuron. Despite its widespread distribution and high levels of expression in mature olfactory neurons, it appears that PHR1 is excluded from the sensory cilia and the absence of PHR1 does not impede olfactory epithelial morphology, development, sensory function, and adaptation. This suggests that either PHR1 does not play a direct role in olfactory function, or other redundant pathways may be compensating in the absence of PHR1. Although best known for phosphoinositide binding, recent studies suggest that PH domain proteins serve a wide range of cellular functions that may be effected through interactions with multiple different binding partners.[11] The exact role for PHR1 in olfactory biology remains to be determined.

Acknowledgments

We wish to thank the laboratory of Dr. R. Reed for advice, technical assistance, some of the antibodies, and the generous use of facilities for EOG recordings and preparing the MeBr-treated animals used in this study. We also wish to acknowledge the Johns Hopkins microscopy core for their assistance in sectioning and preparing the samples for analysis under the electron microscope.

BIBLIOGRAPHY

1. Holbrook EH, Leopold DA. An updated review of clinical olfaction. *Curr Opin Otolaryngol Head Neck Surg* 2006; 14:23–28.
2. Kirk JM, Grant DB, Savage MO, Besser GM, Bouloux PM. Identification of olfactory dysfunction in carriers of X-linked Kallmann's syndrome. *Clin Endocrinol (Oxf)* 1994; 41:577–580.
3. Kulaga HM, Leitch CC, Eichers ER, et al. Loss of BBS proteins causes anosmia in humans and defects in olfactory cilia structure and function in the mouse. *Nat Genet* 2004;36:994–998.
4. Murphy C, Schubert CR, Cruickshanks KJ, Klein BE, Klein R, Nondahl DM. Prevalence of olfactory impairment in older adults. *JAMA* 2002;288:2307–2312.
5. Conley DB, Robinson AM, Shinners MJ, Kern RC. Age-related olfactory dysfunction: cellular and molecular characterization in the rat. *Am J Rhinol* 2003;17: 169–175.
6. Kern RC, Conley DB, Haines GK III, Robinson AM. Pathology of the olfactory mucosa: implications for the treatment of olfactory dysfunction. *Laryngoscope* 2004;114: 279–285.
7. Robinson AM, Conley DB, Shinners MJ, Kern RC. Apoptosis in the aging olfactory epithelium. *Laryngoscope* 2002; 112:1431–1435.
8. Richardson MS. Pathology of skull base tumors. *Otolaryngol Clin North Am* 2001;34:1025–1042, vii.
9. Xu S, Ladak R, Swanson DA, et al. PHR1 encodes an abundant, pleckstrin homology domain-containing integral membrane protein in the photoreceptor outer segments. *J Biol Chem* 1999;274:35676–35685.
10. Kim O, Yang J, Qiu Y. Selective activation of small GTPase RhoA by tyrosine kinase Etk through its pleckstrin homology domain. *J Biol Chem* 2002;277:30066–30071.
11. Lemmon MA. Pleckstrin homology domains: not just for phosphoinositides. *Biochem Soc Trans* 2004;32:707–711.
12. Xu S, Wang Y, Zhao H, et al. PHR1, a PH domain-containing protein expressed in primary sensory neurons. *Mol Cell Biol* 2004;24:9137–9151.
13. Krappa R, Nguyen A, Burrola P, Deretic D, Lemke G. Evectins: vesicular proteins that carry a pleckstrin homology domain and localize to post-Golgi membranes. *Proc Natl Acad Sci U S A* 1999;96:4633–4638.

14. Etournay R, El-Amraoui A, Bahloul A, et al. PHR1, an integral membrane protein of the inner ear sensory cells, directly interacts with myosin 1c and myosin VIIa. *J Cell Sci* 2005;118:2891–2899.
15. Colin C, Baeza N, Bartoli C, et al. Identification of genes differentially expressed in glioblastoma versus pilocytic astrocytoma using Suppression Subtractive Hybridization. *Oncogene* 2006;25:2818–2826.
16. Schwob JE, Youngentob SL, Mezza RC. Reconstitution of the rat olfactory epithelium after methyl bromide-induced lesion. *J Comp Neurol* 1995;359:15–37.
17. Buck LB. Unraveling the sense of smell (Nobel lecture). *Angew Chem Int Ed Engl* 2005;44:6128–6140.
18. Malnic B, Godfrey PA, Buck LB. The human olfactory receptor gene family. *Proc Natl Acad Sci U S A* 2004;101: 2584–2589.
19. Michalakis S, Reisert J, Geiger H, et al. Loss of CNGB1 protein leads to olfactory dysfunction and subciliary cyclic nucleotide-gated channel trapping. *J Biol Chem* 2006;281:35156–35166.
20. McEwen DP, Koenekoop RK, Khanna H, et al. Hypomorphic CEP290/NPHP6 mutations result in anosmia caused by the selective loss of G proteins in cilia of olfactory sensory neurons. *Proc Natl Acad Sci U S A* 2007;104:15917–15922.
21. McClintock TS, Sammeta N. Trafficking prerogatives of olfactory receptors. *Neuroreport* 2003;14:1547–1552.
22. Scholey JM, Anderson KV. Intraflagellar transport and cilium-based signaling. *Cell* 2006;125:439–442.
23. Margolis FL. Olfactory marker protein (OMP). *Scand J Immunol Suppl* 1982;9:181–199.
24. Schwob JE. Neural regeneration and the peripheral olfactory system. *Anat Rec* 2002;269:33–49.
25. Youngentob SL, Kent PF, Margolis FL. OMP gene deletion results in an alteration in odorant-induced mucosal activity patterns. *J Neurophysiol* 2003;90:3864–3873.
26. Youngentob SL, Margolis FL. OMP gene deletion causes an elevation in behavioral threshold sensitivity. *Neuroreport* 1999;10:15–19.